Molecular Mechanisms of the Adsorption of a Model Protein (Human Serum Albumin) on Poly(Methylidene Malonate 2.1.2) Nanoparticles

Yolène Bousquet,[1,3] Pieter J. Swart,[2] Nathalie Schmitt-Colin,[1,3] Florence Velge-Roussel,[3] Mirjam E. Kuipers,[2] Dirk K. F. Meijer,[2] Nicole Bru,[1] Johan Hoebeke,[1,4] and Pascal Breton[1]

Received April 21, 1998; accepted October 14, 1998

Purpose. To understand the molecular mechanisms involved in protein–methylidene malonate 2.1.2 polymer interactions.

Methods. To assess the importance of electrostatic forces in polymer-protein interactions use was made of HSA and its derivatives, which were anionized by succinylation and aconitylation. Surface plasmon resonance measurements, using the three HSA molecules as immobilized ligands and polymer nanoparticles as analytes in the liquid phase, allowed the determination of initial kinetic constants and affinity constants at equilibrium at two different temperatures.

Results. Saturation of binding for the three proteins occurred at approximately 900 protein molecules/nanoparticle. The apparent affinity decreased with increasing electronegativity of the proteins. Surface plasmon resonance measurement of proteins, covalently linked to the chip matrix, showed a high affinity for the nanoparticles ($K_A \approx 10^{10}$ M^{-1}) and confirmed the moderate decrease of affinity with increasing electronegativity of the modified albumins. Measurements at 25 and 37°C showed no significant increase in the albumin-nanoparticle interactions. Dissociation of the proteins from the nanoparticles could only be realized with chaotropic salt solutions.

Conclusions. These results suggest the molecular forces initiating the protein-nanoparticle interactions are mainly of electrostatic nature followed by stabilization by hydrophobic forces. The high affinity confirms the nanoparticles as excellent carriers for protein delivery.

KEY WORDS: nanoparticle; methylidene malonate 2.1.2; protein-polymer interaction; surface plasmon resonance (SPR); albumins.

INTRODUCTION

The increased interest in peptides and proteins as therapeutic or vaccinating agents has prompted the development of biodegradable carriers for their oral and/or parenteral administration in order to avoid proteolytic degradation. Poly(alkylcyanoacrylate) (PACA) nanoparticles have been proposed for the administration of polypeptides like growth hormone releasing factor (1) and for immunoglobulins. Such preparations may enable the targeting of drugs by means of coupling cell-specific antibodies to the drug-carrying nanoparticles (2,3).

Nanoparticles, consisting of poly(methylidene malonate 2.1.2.) (PMM 2.1.2), whose biodegradability, cytotoxicity, and pharmacokinetic properties are promising, have been described (4). These nanoparticles were able to adsorb immunoglobulins to form highly stable immunonanoparticles (5). To analyze the immunoglobulin-nanoparticle interactions, we made use of Surface Plasmon Resonance (SPR) (BIAcore™) (5,6). This method allows the study of interactions in real time between an immobilized reagent and a liquid phase, in which the analyte is dissolved (7).

To characterize the forces which stabilize the nanoparticle-protein interactions at the molecular level, human serum albumin and its succinylated and aconitylated forms (8) are used as model proteins. The varying negative charge of these albumins allows the study of the effect of electrostatic forces in the protein-nanoparticle interactions at physiological pH. Negatively charged albumins exhibit anti-HIV activities through binding to the V3 loop of the envelope protein of HIV-1 gp120 as well as to the T lymphocytes and macrophages as target cells for HIV (9–11). Therefore, these albumins are interesting model compounds. Analysis of the physico-chemical parameters as determined by SPR measurements at different temperatures is used to gain insight into the molecular forces regulating nanoparticle-protein interactions.

MATERIALS AND METHODS

Chemicals

Poly(methylidene malonate 2.1.2) nanoparticles were prepared according to Lescure *et al.* (4). Their mean size, as determined with a N4 nanosizer (Coulter Electronics, Hialeah, FL, USA) was approximately 550 ± 10 nm.

Succinylated and aconitylated human serum albumin (HSA) were prepared as previously described (9). All other reagents used were of analytical grade. Water was of MilliQ (Millipore, Bedford, MA, USA) quality.

Characterization of the Modified HSA

The degree of substitution of the ε-amino groups of the lysines of HSA by succinyl and aconityl residues was determined by the *o*-phthaldialdehyde method (12,13).

The influence of charge on the HSA conformation was assessed by their affinity for a polyclonal rabbit anti-HSA IgG fraction as determined by Surface Plasmon Resonance. Briefly: the rabbit anti-HSA IgG (Sigma Chemicals, St Louis, MI, USA) was immobilized on the sensor chip by a standard procedure (14). HSA solutions in acetate buffer (acetate 10 mM, NaCl 150 mM, EDTA 3.4 mM and surfactant P20 0.05%) from 6.25 to 100 nM were automatically injected at a rate of 5 $\mu l min^{-1}$ for 12 min in the BIAcore™ system. Dissociation of the HSA-antibody complex was followed for 5 minutes before complete desorption with 10 μl of KSCN 3 M. Sensorgrams were analyzed as described in following paragraphs.

[1] Halisol S.A., Paris, France.

[2] Groningen Utrecht Institute for Drug Exploration (GUIDE), Department of Pharmacokinetics and Drug Delivery, University Center for Pharmacy, Groningen, The Netherlands.

[3] CJF93/09 INSERM "Immunologie des Maladies Parasitaires," UFR Sciences Pharmaceutiques, Université François Rabelais, Tours, France.

[4] To whom correspondence should be addressed. (e-mail: hoebeke@ibmc.u-strasbg.fr)

0724-8741/99/0100-0141$16.00/0

Biosensor Experiments

The BIAcore™ 1000 upgraded system was from Pharmacia Biosensor AB (Uppsala, Sweden). Sensor chips CM5, surfactant P20, the thiol-coupling kit containing N-ethyl-N'-(3-diethylaminopropyl) carbodiimide (EDC), N-hydroxysuccinimide (NHS), 2-(2-pyridinyldithio)ethane-amine (PDEA), and the eluent buffer, HBS (HEPES 10 mM, NaCl 150 mM, surfactant P20 0.05%, pH 7.4) were supplied by Pharmacia.

Protein Immobilization on Sensor Surfaces

Because most of the amine groups in succinylated or aconitylated HSA are substituted, it was decided to bind native and modified HSA by the thiol-coupling method (see Reaction Scheme I) taking advantage of the single free sulfhydryl group present in these proteins.

After equilibration with HBS, the following sample injections were done: (i) equal volumes of a solution of NHS (0.1 M in water) and EDC (0.4 M in water) were first mixed and 10 µl were injected to activate the carboxylated dextran; (ii) 20 µl of a PDEA solution (0.08 M) in borate buffer 0.1 M pH 8.5 were injected for chemical modification; (iii) 35 µl of HSA or one of its modified forms in acetate buffer (10 mM) at 200 μgml^{-1} were injected for immobilization. The free cysteyl residues of the HSAs were first reduced using 1 mM DTT solutions; (iv) the remaining PDEA molecules were displaced by 10 µl of a cysteine solution (1 M) in water. The immobilization protocol was performed within 30 min with a continuous flow of 5 $\mu lmin^{-1}$ of HBS.

Binding Assays onto Protein-Covered Sensor Chips

Binding/elution cycles were performed at 25°C at 5 $\mu lmin^{-1}$. Nanoparticle suspensions of 8, 4, 2, 1, and 0.5 $mgml^{-1}$ in HBS were injected for 5 min and allowed to dissociate for another 5 min in eluent buffer, to allow to calculate for association rate and dissociation rate constants of the interaction. After the dissociation phase, the sensor chip was regenerated by 10 µl of KSCN 3 M.

Regeneration Assays After Nanoparticle Interactions

As shown previously (5), the desorption of nanoparticles from protein immobilized on the sensor chip was not achieved with 0.1 M HCl. To be able to use several times more the same immobilized protein, several chaotropic reagents were tested to achieve maximal desorption of the nanoparticles.

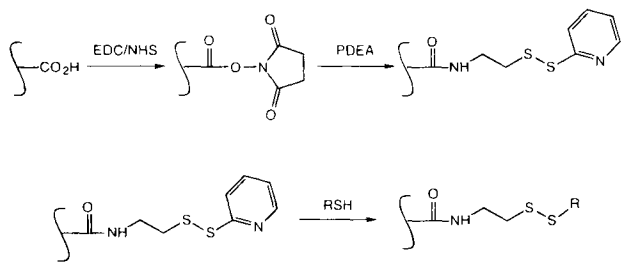

Scheme I.

Temperature Dependency of the Protein-Nanoparticle Interaction

Binding assays, as described in the previous paragraph, were also performed at 37°C to further evaluate HSA-nanoparticle interactions.

Analysis of the Sensorgrams

Sensorgrams were analysed by the BIAevaluation software from Pharmacia using the equations for homogeneous kinetics of a simple A + B ↔ AB reaction. [15]. Dissociation rate constants (k_{off}) and association rate constants (k_{on}) can be calculated.

The affinity constants were determined as $K_A = k_{on}/k_{off}$.

Preparation and Characterization of Proteo-Nanoparticles

A nanoparticle suspension at 10 $mgml^{-1}$ was added to 1 ml of native or modified HSA (20–400 μgml^{-1}) in phosphate buffer pH 7.4. The mixture was shaken for 2 h at room temperature on a IKA Vibrax VXR (Jankel and Kunkel, Staufen, Germany). Proteo-nanoparticles were ultracentrifuged for 5 min at 540,000 *g* and the protein content of the supernatant was determined by HPLC, using a Protein C4 column (250 mm × 2.1 mm) (Vydac, Hesperia Ca, USA) with an integrated type 1090 series II chromatograph (Hewlett Packard, Les Ulis, France).

Proteins eluted with a 13-min linear acetonitrile/water gradient (from 65% to 45% water) containing trifluoroacetic acid 0.05% were detected at 210 nm. Calibration was performed by HSA and modified HSA (10 to 400 μgml^{-1}) processed as for their adsorption on nanoparticles.

The molarity of nanoparticles was calculated as

$$[Np] = W \times 7.7 \times 10^{14}/N \times 10 \quad (1)$$

in which W is the concentration of nanoparticles in $mgml^{-1}$, N is the Avogadro number and 7.7×10^{14} is the number of particles in a suspension of 10 $mgml^{-1}$ (6).

RESULTS

Characterization of the Modified Human Serum Albumins

Figure 1 shows the calibration of native, succiniylated and aconitylated HSA with the amino reagent, *o*-phthaldialdehyde. Using the equation

$$\partial = 35\ (1 - b/a) \quad (2)$$

in which 35 is the number of accessible amino groups in native HSA (16), ∂ is the number of modified amino groups, a the slope of the calibration curve for native HSA and b the slope of the calibration curve for the modified HSA respectively, the amount of added negative charges could be calculated. Succinylation removes protonizable amino groups and at the same time adds one carboxylic acid group per reacted amino group (charge difference is −2 per reacting amino group). In the case of a reaction with aconitic anhydride, the charge difference is −3 negative charges per substituted amino group.

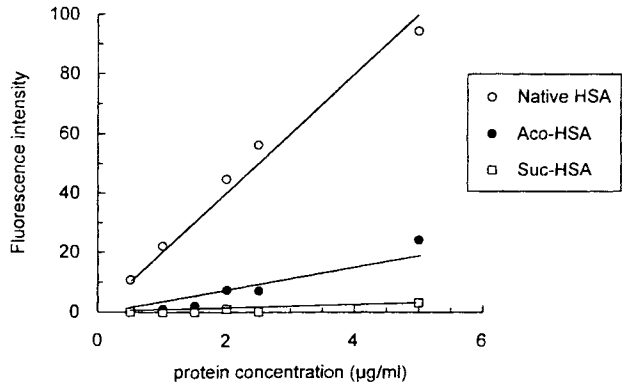

Fig. 1. Quantitation of substituted amino groups in aconitylated HSA (Aco-HSA) and succinylated HSA (Suc-HSA). For each protein, free amino groups were modified with *o*-phthaldialdehyde and the fluorescence measured for different protein concentrations. From the slope of the plots, the amount of substitution was calculated according to Eqn (2). Obviously, substitution of standard native HSA was nihil.

With the batches experimented, succinylation modified 34 lysine residues, increasing the charge with −68 units; aconitylation modified 28 residues, increasing the charge of aconitylated HSA with −84 units/molecule.

Using SPR measurements at 25°C, the apparent affinity constants for the interaction between a polyclonal rabbit anti-HSA IgG was determined as 3.2 ± 1.3. 10^9 M^{-1} for native HSA, 1.3 ± 0.8. 10^9 M^{-1} for the succinylated form and 3.8 ± 2.3. 10^9 M^{-1} for the aconitylated form. Standard deviations were calculated from the linearisation of the saturation binding curve using the RU values bound at equilibrium (R_{eq}) at different concentrations.

Quantitative Analysis of HSA-Bound Nanoparticles

Binding of native and modified HSA shows a clear saturation pattern as a function of added protein (Fig. 2). Table I summarizes the HSA concentrations needed for 50% saturation and maximal number of HSA/nanoparticle calculated from the saturation curves. Negatively charged HSA reached half-saturation at higher concentrations than the native one while the number of molecules HSA/nanoparticle was slightly increased.

Table I. Affinity Constants and Maximal Binding of HSA as Calculated from HPLC Analysis

HSA	Half saturation molecules HSA/nanoparticle µM	B_{max}
Native	2.3 ± 0.8[a]	1094 ± 162[b]
Succinylated	5.0 ± 1.9	1562 ± 365
Aconitylated	6.8 ± 2.1	1719 ± 357

[a] The concentration to reach half saturation was calculated from the saturation binding curves shown in Fig. 1 using Grafit (Erithacus Software, Staines, UK) for a binding isotherm.

[b] The maximal amount of molecules of HSA bound/nanoparticle was calculated from the B_{max} value obtained by the Multifit program and from the molarity of nanoparticles calculated from Equation (1).

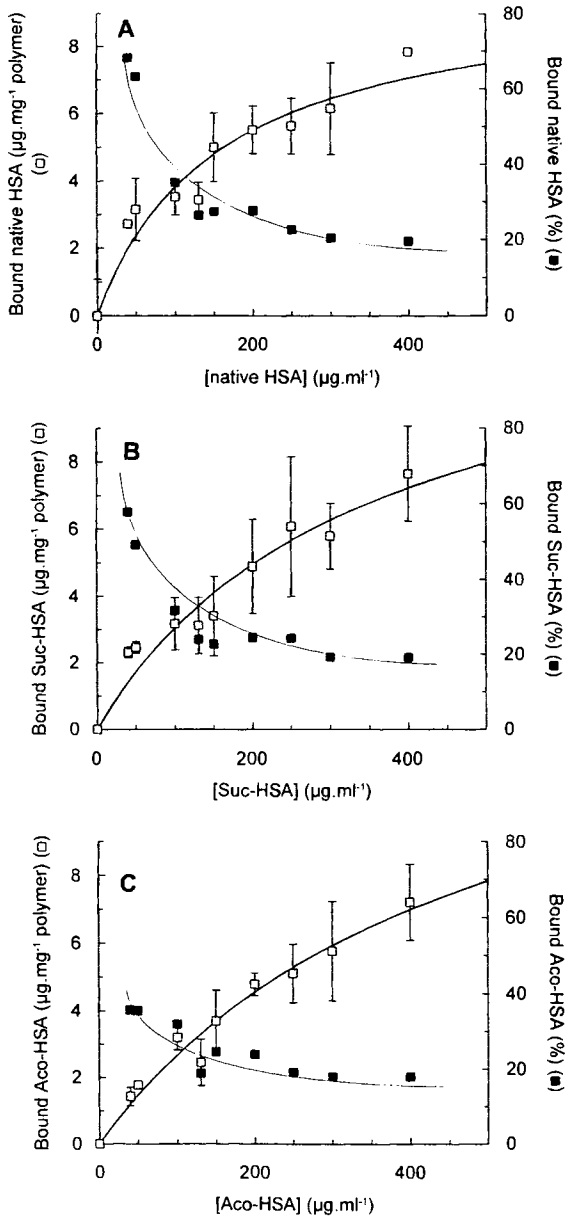

Fig. 2. Adsorption of HSA (A), succinylated HSA (Suc-HSA) (B), or aconitylated HSA (Aco-HSA) (C) onto poly(methylidene malonate 2.1.2) nanoparticles. Unbound proteins in the supernatants of the nanoparticles were quantified by HPLC. The adsorbed protein was calculated as the difference of protein amount in the supernatant after and before the adsorption. The results are expressed as µg proteinmg^{-1} nanoparticles (□ – □) or % adsorbed protein (■ – ■). Lines were fitted for a normal Langmuir binding.

Interaction of Nanoparticles with HSA Studied by Surface Plasmon Resonance

Immobilization of the HSA molecules on the sensorchip decreased as a function of their negative charges (Table II). This was expected since the negatively charged carboxylated dextran matrix is repulsive for net negatively charged macromolecules. Figure 3 shows the sensorgrams for binding of 1

Table II. Immobilization of the HSA Proteins on the Matrix of the Sensorchip and Interaction with 0.12 nM Nanoparticles

HSA	Immobilization ($ng.mm^{-2}$)[a]	Ratio $boundHSA_{mod}/boundHSA_{nat}$	Nanoparticles ($ng.mm^{-2}$)	Ratio nanoparticles/HSA
Native	3.24	1	1.66	0.512
Succinylated	1.96	0.60	0.68	0.347
Aconitylated	0.69	0.21	0.28	0.407

[a] Calculated as 1000 RU for 1 $ngmm^{-2}$ of the sensor chip.

Table III. Kinetic Constants of the Interaction Between Nanoparticles and Human Serum Albumins

	0.12 nM nanoparticles			0.51 nM nanoparticles		
HSA	k_{off} (s^{-1}) × 10^3	$k_{on}(M^{-1}s^{-1}) \times 10^{-6}$	$K_A(M^{-1}) \times 10^{-9}$	$k_{off}(s^{-1}) \times 10^3$	$k_{on}(M^{-1}s^{-1}) \times 10^{-6}$	$K_A(M^{-1}) \times 10^{-9}$
Native	1.58	7.4	4.7	1.13	8.5	7.5
Succinylated	1.96	11.5	5.9	2.42	8.0	3.3
Aconitylated	2.27	3.5	1.5	3.47	4.9	1.4

Note: Dissociation rate constants (k_{off}) and association rate constants (k_{on}) were calculated from the sensorgrams as described under Materials and Methods. The affinity constant (K_A) was calculated as k_{on}/k_{off}.

$mgml^{-1}$ nanoparticles (0.12 nM) on respectively native, succinylated and aconitylated HSA. Increased negativity of the immobilized HSA molecules resulted in a smaller amount of nanoparticles adsorbed. Calculating the R_{eq} values of nanoparticles bound, the ratio of binding to the modified HSAs, was itself somewhat less than particle bound modified HSA (Table II). This suggests the decrease in binding is not only due to the lesser amounts of modified HSAs immobilized.

Analysis of the kinetic constants for the binding of nanoparticles at 0.12 and 0.51 nM showed association rate constants which were similar for the native and succinylated form of HSA but was lower for the aconitylated HSA. The dissociation rate constants increased with the increase of the negativity of the proteins (Table III). Nanoparticles (0.51 nM) were run at different flow rates (from 2 to 50 $\mu lmin^{-1}$). No significant changes in the association rate were observed excluding mass-transfer influences (data not shown).

Temperature Dependency of the HSA-Nanoparticle Interactions

To study the thermodynamics of the HSA-nanoparticle interactions, saturation binding experiments were performed at

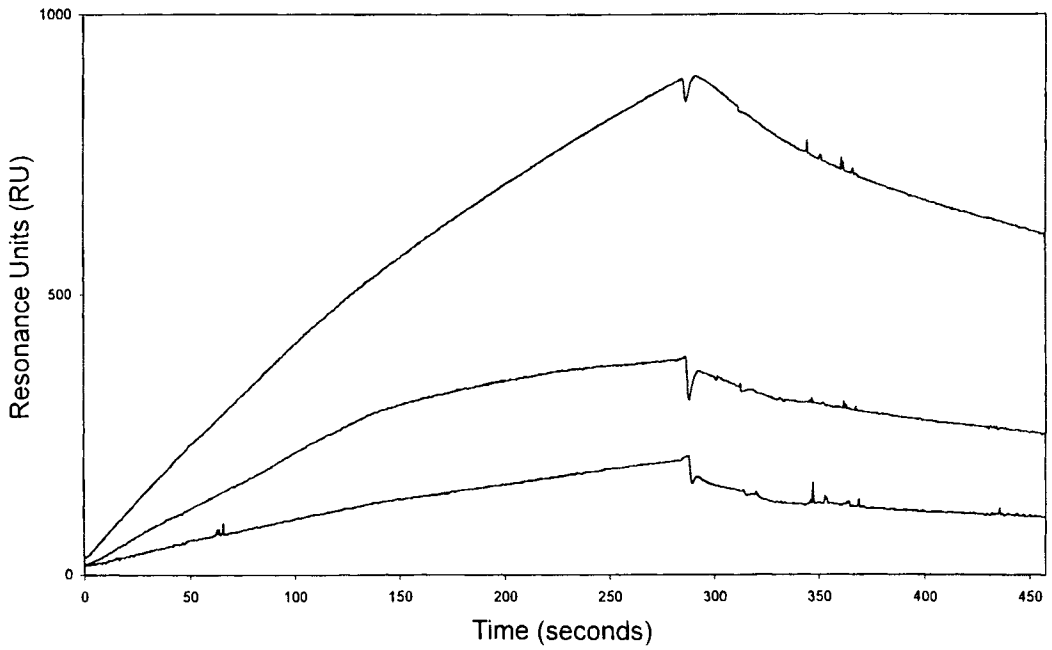

Fig. 3. Sensorgrams of the adsorption of 0.12 nM nanoparticles at 25°C on HSA (upper curve), succinylated HSA (middle curve) and aconitylated HSA (lower curve). Nanoparticles were injected at 5 $\mu lmin^{-1}$ for 5 min (association phase) and replaced by HBS buffer for 2 min (dissociation phase).

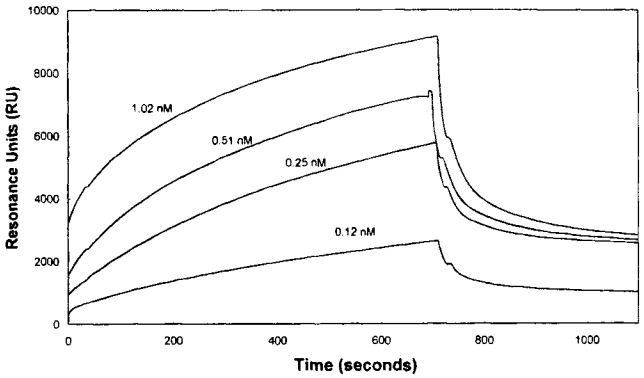

Fig. 4. Sensorgrams of the adsorption of nanoparticles at increasing concentrations (0.12–1.02 nM) at 37°C on HSA. Nanoparticles were injected at 5 $\mu l min^{-1}$ for 12 min and allowed to dissociate in HBS buffer for 4 min.

two different temperatures (25 and 37°C). The sensorgrams of this experiment at 37°C are illustrated in Fig. 4. As may be expected, both association rate and dissociation rate constants increased with the temperature (Table IV). Since association rate and dissociation rate constants increased in a similar ratio, the affinity constant at both temperatures did not show a significant difference, indicating the reaction is not enthalpy driven. The possibility of the use only of two temperatures and the dispersion of the K_A values are improper for more sophisticated thermodynamic analysis.

Desorption of HSA from Nanoparticles

In previous experiments, it was shown the commonly used desorbent HCl 0.1 M, was inefficient to dissociate the nanoparticles from proteins immobilized on the sensor chip (5). Since the experiments described here suggest extra negative charges on the protein decrease the affinity for the nanoparticles, protonation of the protein with HCl, is likely to be inadequate for the dissociation of protein-nanoparticle complexes. Other chaotropic agents were thus tested to desorb the nanoparticles from the immobilized proteins. As shown in Table V, both $MgCl_2$ 3 M and KSCN 3 M could regenerate the sensorchip, KSCN 3 M being the most efficient chaotropic agent. Glycine buffer 0.2 M at pH 2.8 had no effect at all. To increase the electronegativity of the adsorbed proteins, assays were performed with NaOH 0.1 M. However, this alkaline solution disrupted the disulfide bond between the immobilized proteins, and the matrix was unsuitable for further experiments (see Reaction scheme).

Table V. Desorption of Proteins from Nanoparticles

Chaotropic agents[a]	$MgCl_2$ 3 M	KSCN 3 M	Glycine 0.2 M pH 2.8	NaOH 0.1 M
% desorption[b]	24	64	0	−284[c]

[a] Chaotropic agents were injected for 2 min at 5 $\mu l min^{-1}$ after adsorption of 0.25 nM nanoparticles on HSA.

[b] % is calculated as the ratio of $(RU_b - RU_r/RU_b - RU_{bl})$ in which RU_b is the value after adsorption of the nanoparticles, RU_r is the value after passage of the chaotropic agent, RU_{bl} is the value before adsorption of the nanoparticles.

[c] The negative value is due to desorption of the immobilized HSA from the matrix (see text).

Decrease in Resonance Units after desorption could, in principle, be due to two phenomena: (i) elution of the intact nanoparticles from the matrix and/or (ii) solubilization of the nanoparticles merely preserving an association of monomers or oligomers with the immobilized proteins. Assuming the physico-chemical conditions and dynamics responsible for the observed phenomena at the sensor-chip surface might be transposed to bulk colloid suspensions, nanoparticle stability was monitored by turbidity measurements at 540 nm in a spectrophotometer in the different desorption solutions mentioned above. The data shown in Table VI, did not reveal any time-dependent or medium-dependent decrease in turbidity for nanoparticles suspended for 2 h in any of the tested media. Contrary to what Breton et al. proposed (5), such a result would exclude the second hypothesis and confirm the intact nanoparticles were desorbed from immobilized proteins in the course of the dissociation phase or during regeneration of the sensor chip.

DISCUSSION

Protein adsorption onto polymeric surfaces has been extensively used for diagnostic (immunoassays on polystyrene plates or latex particles) or therapeutic purposes. The molecular forces underlying this adsorption are generally supposed to be hydrophobic (17). Söderquist and Walton (18) proposed a three-stage mechanism in which the initial binding step could result from weak and reversible interactions, followed by a much stronger and irreversible interaction leading to slow conformational changes of proteins. While the irreversible phases are generally accessible to experimental study over a long time, as shown in the binding experiments (Fig. 2), the initial steps leading to irreversible adsorption are more difficult to investigate experimentally.

Table IV. Temperature Dependency of HSA–Nanoparticle Interactions

	25°C			37°C		
[Np] nM	k_{off} (s^{-1}) × 10^3	k_{on} ($M^{-1} s^{-1}$) × 10^{-6}	K_A (M^{-1}) × 10^{-9}	k_{off} (s^{-1}) × 10^3	k_{on} ($M^{-1} s^{-1}$) × 10^{-6}	K_A (M^{-1}) × 10^{-9}
0.12	0.33	6.5	19.7	0.76	7.2	9.5
0.25	0.38	3.6	9.5	0.93	4.7	5.1
0.51	0.39	4.1	10.6	1.37	5.4	3.9
1.02	0.51	2.6	5.2	1.66	13.1	7.9
Mean ± S.D.	0.39 ± 0.08	4.2 ± 1.6	11.2 ± 6.0	1.18 ± 0.41	7.6 ± 3.8	6.6 ± 2.5

We have shown previously Surface Plasmon Resonance could be used to study protein-nanoparticle interactions using poly(methylidene malonate 2.1.2. nanoparticles) (5,6). Since this method allows the real-time analysis of interactions occurring between molecular species, it is especially useful to study the initial kinetics of protein-nanoparticle interactions. We therefore decided to focus on a model protein, human serum albumin, and its modified succinylated and aconitylated forms. Addition of 68 and 84 negative charges to the HSA, with the succinyl and the aconityl residues respectively, hardly affected the molecular weight or the conformation of the HSA molecules, as was assessed by the immunological integrity of the modified forms. The model proteins used were thus suitable to study the influence of electrostatic interactions on the protein-nanoparticle complex formation.

The association rate constants calculated for the three different HSA are quite high ($\pm 10^7\ M^{-1}\ s^{-1}$). Calculating the rate of a diffusion-controlled reaction as (19):

$$k_{on} = \frac{2RT}{3\eta}\left(\frac{1}{r_A} + \frac{1}{r_B}\right)(r_A + r_B) \qquad (3)$$

in which R is the universal gas constant, T 298K, η the viscosity of water, r_A 2.10^{-9} m (radius of HSA) and r_B 275.10^{-9} m (radius of the nanoparticle), the association rate constant of HSA-nanoparticle interaction is $2.2 \times 10^8\ M^{-1}\ s^{-1}$. Taking into account the loss of degrees of liberty of one of the reagents (HSA) which is immobilized and the non-ideal semi-liquid matrix of the sensor chip, the observed apparent association rate constant (10 times lower than the calculated rate constant) is compatible with a diffusion-controlled reaction. This also explains the similarity of the observed k_{on} for the three HSA modalities studied and suggests conformational changes do not play a role in the protein-nanoparticle interaction.

The decrease of affinity with increase of the negative charges seems to be mainly due to an increase of the dissociation rate constant, suggesting electronegativity decreases the stability of the protein-nanoparticle-complex and thus, the relative impact of electrostatic interactions. These results are compatible with the HPLC experiments (Table I), which also show a slightly higher overall apparent affinity for native HSA compared to the succinylated or aconitylated form.

This hypothesis received confirmation by the independence of the affinity constants with the temperature. This suggests that the reaction is not enthalpy-driven. The main force, driving the reaction to complex formation may be the entropy. This suggests the existence of electrostatic interaction since neutralisation of positive and negative forces in water induce an enthalpy change around 0 and positive entropy changes due to disruption of the ordered water layers around the ions (20).

Further proof of the importance of electrostatic interactions was given by the desorption studies of the complex. As previously shown (5), it was confirmed here that acidification did not result in desorption. Since acidification should normally increase the positive charges of HSA, it could increase the affinity of the protein for the nanoparticles in contrast to the negative influence of protein-nanoparticle stability by increasing the anionic state of the proteins. Yet, high concentrations of salt such as $MgCl_2$ and KSCN, which are supposed to destroy the electrostatic interactions by ion exchange, were able to dissociate the protein-nanoparticle complex. This points again to a crucial role of electrostatic interactions. It must be noted however, these chaotropic agents can also disrupt hydrophobic forces.

The initial interaction between poly(methylidene malonate 2.1.2) nanoparticles and proteins should be thus determined by the interaction of positively charged residues on the protein with the negatively charged nanoparticle. Although the polymer carries no charges, it has been shown that the nanoparticles have a slightly negative zeta potential (unpublished data) which could be due to the generation of carboxylate residues by hydrolysis of the polymer side chains (4,21). Previous findings which showed a relatively higher adsorption of IgG than of bovine serum albumin to the nanoparticles, when a mixture of the two proteins were used, were ascribed to interaction with the more hydrophobic Fc fragment of IgG (5). An alternative explanation according to the mainly electrostatic nature of protein-nanoparticle interactions could be the higher pI value of IgG (between 7 and 8) compared to bovine serum albumin (pI = 5.4).

It must be emphasized that SPR measurements only study the initial reversible steps in the interactions between nanoparticles and proteins. The high stability of protein-nanoparticle complexes which was previously shown (5) probably involves conformational changes of the protein, finally leading to an increase of hydrophobic interactions or hydrogen bonds with the ester oxygens of the polymer and making the adsorption irreversible.

The adsorption mechanisms analyzed here are not only typical for the poly(methylidene) malonate nanoparticles since similar findings were observed with polyisobutyl cyanoacrylate nanoparticles (22). They should have practical applications for the use of these nanoparticles as protein carriers. Protein or peptide adsorption should be done preferentially at a pH below their pI values. The protein-nanoparticles should be stable even at the acidic pH conditions of the stomach, making them interesting candidates for oral delivery, if enzymatic proteolysis can be avoided.

Table VI. Stability of the Nanoparticles in the Different Regenerating Solutions

Solution	HBS	$MgCl_2$ 3M	KSCN 3M	Glycine 0.2M pH = 2.8
t = 0	0.527[a]	0.479	0.490	0.554
t = 2 h	0.695	0.586	0.627	0.699

[a] Values correspond to the absorbance at 540 nm (turbidity) of a suspension of 0.51 nM nanoparticles in the different solutions directly after dilution and two hours after dilution.

REFERENCES

1. J. C. Gautier, J. L. Grangier, A. Barbier, P. Dupont, D. Dussossoy, G. Pastor, and P. Couvreur. Biodegradable nanoparticles for subcutaneous administration of growth hormone releasing factor (hGRF). *J. Contr. Rel.* **20**:67–77 (1992).
2. L. Illum, P. D. E. Jones, J. Kreuter, R. W. Baldwin, and S. S. Davis. Adsorption of monoclonal antibodies to polyhexylcyanoacrylate nanoparticles and subsequent immunospecific binding to tumour cell in vitro. *Int. J. Pharm.* **17**:65–76 (1983).

3. C. Kubiak, L. Manil, and P. Couvreur. Sorptive properties of antibodies onto cyanoacrylic nanoparticles. *Int. J. Pharm.* **41**:181–187 (1988).
4. F. Lescure, C. Seguin, P. Breton, P. Bourrinet, D. Roy, and P. Couvreur. Preparation and characterization of novel poly(methylidene malonate 2.1.2.)-made nanoparticles. *Pharm. Res.* **11**:1270–1277 (1994).
5. P. Breton, X. Guillon, D. Roy, S. Tamas, L. Marchal-Heussler, N. Bru, and F. Lescure. Evaluation of the interaction between poly(methylidene malonate 2.1.2) nanoparticles and an anti-CD4 by surface plasmon resonance (SPR). *Eur. J. Pharm. Biopharm.* **43**:95–103 (1996).
6. F. Velge-Roussel, P. Breton, X. Guillon, F. Lescure, N. Bru, D. Bout, and J. Hoebeke. Immunochemical characterization of antibody-coated nanoparticles. Experientia **52**:803–806 (1996).
7. M. Malmqvist. Biospecific interaction-analysis using biosensor technology. *Nature* **361**:186–187 (1993).
8. P. J. Swart and D. K. F. Meijer. Negatively-charged albumins: a novel class of polyanionic proteins with a potent anti-HIV activity. *Int. Antiviral News* **2**:69–71 (1994).
9. R. W. Jansen, G. Molema, R. Pauwels, D. Schols, E. de Clercq, and D. K. F. Meijer. Potent *in vitro* anti-human immunodeficiency virus-1 activity of modified human serum. *Mol. Pharmacol.* **39**:818–823 (1991).
10. R. W. Jansen, D. Schols, R. Pauwels, E. De Clercq, and D. K. F. Meijer. Novel, negatively charged, human serum albumins display potent and selective *in vitro* anti-human immunodeficiency virus type I activity. *Mol. Pharmacol.* **44**:1003–1007 (1993).
11. M. E. Kuipers, J. G. Huisman, P. J. Swart, M-P. de Béthune, R. Pauwels, H. Schuitemaker, E. de Clercq, and D. K. F. Meijer. Mechanisms of anti-HIV activity of negatively charged albumins: biomolecular interaction with the HIV-1 envelope protein gp120. *J. Acq. Immune Def. Syn. Human Retrovir.* **11**:419–429 (1996).
12. V. K. Sveda, I. J. Galaev, I. L. Borisov, and I. V. Berezin. The interaction of amino acids with *o*-phthaldialdehyde: a kinetic study and spectrophotometric assay of the reaction product. *Biochemistry* **101**:188–195 (1980).
13. B. N. Jones, S. Pääbo, and S. Stein. Amino acid analysis and enzymatic sequence determination of peptides by an improved o-phthaldialdehyde precolumn labeling procedure. *J. Liq. Chromatogr.* **4**:565–586 (1981).
14. B. Johnsson, S. Löfås, and G. Lindquist. Immobilization of proteins to a carboxymethyldextran-modified gold surface for biospecific interaction analysis in surface plasmon resonance sensors. *Anal. Biochem.* **198**:268–277 (1991).
15. BIAevaluation 2.1 Software Handbook. pp A-2 to A-4. Pharmacia Biosensor AB, Uppsala, Sweden (1995).
16. S. Muller. Peptide-carrier conjugation. in M. H. V. van Regenmortel, J. P. Briand, S. Muller, and S. Plaué (Eds), *Synthetic polypeptides as antigens*, Elsevier, Amsterdam, 1988, pp. 95–130.
17. P. Bagchi and S. M. Birnbaum. Effect of pH on the adsorption of immunoglobulin G on anionic poly(vinyltoluene) model latex particles. *J. Colloid Interface Sci.* **83**:460–478 (1981).
18. M. E. Söderquist and A. G. Walton. Structural changes in proteins adsorbed on polymer surfaces. *J. Colloid Interface Sci.* **75**:386–397 (1980).
19. M. Eigen. Diffusion control in biochemical reactions. In S. C. Mintz and S. M. Widmayer (eds), *Quantum Statistical Mechanisms in the Natural Sciences*, Plenum Press, New York, 1973, pp. 37–61.
20. P. D. Ross and S. Subramanian. Thermodynamics of protein association reactions: forces contributing to stability. *Biochemistry* **20**:3096–3102 (1981).
21. D. Roy, X. Guillon, F. Lescure, P. Couvreur, N. Bru, and P. Breton. On shelf stability of freeze-dried poly(methylidene malonate 2.1.2) nanoparticles. *Int. J. Pharm.* **148**:165–175 (1997).
22. J. C. Olivier, C. Vauthier, M. Taverna, D. Ferrier, and P. Couvreur. Preparation and characterization of biodegradable polyisobutyl cyanoacrylate nanoparticles with the surface modified by the adsorption of proteins. *Colloids Surfaces B: Biointerfaces* **4**:349–356 (1995).